Inorg. Chem. **2005**, *44*, 9305–9313

Remote and Adjacent Excited-State Electron Transfer at TiO_2 Interfaces Sensitized to Visible Light with Ru(II) Compounds

Feng Liu and Gerald J. Meyer*

Departments of Chemistry and Materials Science and Engineering, Johns Hopkins University, Baltimore, Maryland 21218

Received August 4, 2005

The ruthenium polypyridyl compounds, $Ru(dpp)_2(deeb)(PF_6)_2$ (**Ru-deeb**) and *cis*-$Ru(dpp)_2(eina)_2(PF_6)_2$ (**Ru-eina**), where dpp is 4,7-diphenyl-1,10-phenanthroline, deeb is 4,4′-diethyl ester-2,2′-bipyridine, and eina is 4-ethyl ester pyridine, have been prepared and characterized to sensitize nanocrystalline TiO_2 (anatase) thin films. In neat acetonitrile at room temperature, **Ru-deeb** was emissive with $\lambda_{em} = 675$ nm, $\tau = 780$ ns, and emission quantum yield $\phi_{em} = 0.067$, whereas **Ru-eina** was nonemissive with $\tau < 10$ ns. The short lifetime and observed photochemistry for **Ru-eina** are consistent with the presence of low-lying ligand-field (LF) excited states. The metal-to-ligand charge transfer (MLCT) excited states of **Ru-deeb** were found to be localized on the surface-bound deeb ligand, and on the remote dpp ligand for **Ru-eina**. Interfacial proton concentration was employed to tune the relative sensitizer–semiconductor energetics. Injection quantum yields, ϕ_{inj}, varied from ~0.2 at pH = 5 to ~1 at pH = 1, with a slope of ~0.15/pH for both compounds. At pH = 12, long-lived excited states were observed with $\phi_{inj} < 0.05$. At pH ≤ 2, ϕ_{inj} became temperature-dependent for **Ru-eina**, but not for **Ru-deeb**. A mechanism is proposed wherein population of LF states at elevated temperatures lowers ϕ_{inj}.

Introduction

The study of the interfacial electron transfer between molecular adsorbates and semiconductor nanoparticles is presently under intense investigation.[1] In dye-sensitized solar cells, the quantum yield for excited-state electron transfer to the semiconductor, ϕ_{inj}, is a critical parameter for the production of electrical power. It is therefore desirable to have a mechanistic understanding of the molecular factors that influence ϕ_{inj}. Excited-state electron injection from transition-metal compounds anchored to TiO_2 surfaces is known to take place on a pico- to femtosecond time scale under many experimental conditions.[2−7] For the metal-to-ligand charge transfer (MLCT) excited states of the well-studied *cis*-$Ru(dcb)_2(NCS)_2$, where dcb is 4,4′-$(COOH)_2$-2,2′-bipyridine, the current thinking is that ultrafast injection occurs from the singlet excited state whereas the slower injection occurs from the triplet state.[5] Studies with Os(II) sensitizers support this general model.[6]

There is also some evidence that the slower triplet injection occurs when light excitation promotes an electron to a ligand that is not directly bound to the semiconductor surface.[5b] Introduction of a methylene, phenyl, or phenyl ethyne spacer between the surface anchoring group and the diimine ligand has been shown to tune ϕ_{inj} and/or the injection rate constants.[7−10] In light of these literature observations, a significant effect on ϕ_{inj} and the power conversion efficiency

* To whom correspondance should be addressed. Email: meyer@jhu.edu.

(1) (a) Grätzel, M. *Nature* **2001**, *414*, 338. (b) Watson, D. F.; Meyer, G. J. *Annu. Rev. Phys. Chem.* **2005**, *56*, 119.
(2) (a) Tachibana, Y.; Moser, J. E.; Grätzel, M.; Klug, D. R.; Durrant, J. R. *J. Phys. Chem.* **1996**, *100*, 20056. (b) Haque, S. A.; Palomeras, E.; Cho, B. M.; Green, A. N. M.; Hirata, N.; Klug, D. R.; Durrant, J. R. *J. Am. Chem. Soc.* **2005**, *127*, 3456.
(3) Hannappel, T.; Burfeindt, B.; Storck, W.; Willig, F. *J. Phys. Chem. B* **1997**, *101*, 6799.
(4) Asbury, J. B.; Ellingson, R. J.; Ghosh, H. N.; Ferrere, S.; Nozik, A. J.; Lian, T. *J. Phys. Chem. B* **1999**, *103*, 3110.
(5) (a) Benko, G.; Kallioinen, J.; Korppi-Tommola, J. E. I.; Yartsev, A. P.; Sundström, V. *J. Am. Chem. Soc.* **2002**, *124*, 489. (b) Benko, G.; Kallioinen, J.; Myllyperko, P.; Trif, F.; Korppi-Tommola, J. E. I.; Yartsev, A. P.; Sundström, V. *J. Phys. Chem. B* **2004**, *108*, 2862.
(6) Kuciauskas, D.; Monat, J. E.; Villahermosa, R.; Gray, H. B.; Lewis, N. S.; McCusker, J. K. *J. Phys. Chem. B* **2002**, *106*, 9347.
(7) Piotrowiak, P.; Galoppini, E.; Wei, Q.; Meyer, G. J.; Wiewior, P. *J. Am. Chem. Soc.* **2003**, *125*, 5258.
(8) (a) Heimer, T. A.; D'Arcangelis, S. T.; Farzad, F.; Stipkala, J. M.; Meyer, G. J. *Inorg. Chem.* **1996**, *35*, 5319. (b) Gillaizeau-Gauthier, I.; Odobel, F.; Alebbi, M.; Argazzi, R.; Costa, E.; Bignozzi, C. A.; Qu, P.; Meyer, G. J. *Inorg. Chem.* **2001**, *40*, 6073.
(9) Asbury, J. B.; Hao, E.; Wang, Y. Q.; Ghosh, H. N.; Lian, T. Q. *J. Phys. Chem. B* **2001**, *105*, 4545.
(10) Wang, D.; Galoppini, E.; Hoertz, P. G.; Carlisle, R. A.; Meyer, G. J. *J. Phys. Chem. B* **2004**, *108*, 16642.

10.1021/ic0513336 CCC: $30.25
Published on Web 11/10/2005

Scheme 1

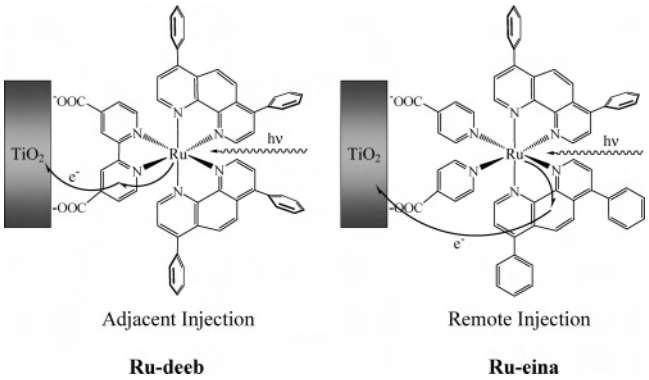

might be expected when the excited state is localized on a ligand that is remote to the semiconductor surface relative to one that is adjacent,[11] Scheme 1.

In this paper, two ruthenium polypyridyl compounds, $Ru(dpp)_2(deeb)(PF_6)_2$ (**Ru-deeb**) and *cis*-$Ru(dpp)_2(eina)_2(PF_6)_2$ (**Ru-eina**), where dpp is 4,7-diphenyl-1,10-phenanthroline, deeb is 4,4′-diethyl ester-2,2′-bipyridine, and eina is 4-COOEt-pyridine, have been specifically prepared to study remote and adjacent interfacial electron injection (Scheme 1). The results demonstrate nearly quantitative remote excited-state electron injection yields and high photon-to-current efficiencies. The possible role(s) of ligand-field excited states at these sensitized interfaces is also described.

Experimental Section

Materials. 4,7-Diphenyl-1,10-phenanthroline (97%), ethyl isonicotinate (98%), titanium(IV) isopropoxide, zirconium(IV) propoxide (70%), iodine (99.999%), LiI (99.9%), LiCl (99%), and NH_4PF_6 (95%) from Aldrich were used as received. $RuCl_3 \cdot xH_2O$ was obtained from Johnson Matthey. Electrochemical grade tetrabutylammonium perchlorate (TBAP) from Fluka was recrystallized in EtOH before use. Burdick and Jackson spectroscopic-grade acetonitrile was used as received. All solvents for synthesis and purification were of reagent grade or better.

Materials Preparations. Mesoporous TiO_2 and ZrO_2 thin films were prepared by sol−gel techniques previously described.[12] For photo-electrochemical measurements, the TiO_2 particles were deposited onto fluorine-doped tin oxide conductive glass (Libby-Owens Ford). For spectroscopic measurements, the TiO_2 particles were deposited onto microscope slides (ca. $50 \times 12.5 \times 1$ mm^3; VWR) that could be inserted diagonally into a 1 cm path length quartz cell. For acid- and base-treated TiO_2, the films were placed in aqueous solutions of known pH (adjusted with H_2SO_4 or NaOH) for 30 min. The films were then removed, washed with copious amounts of acetonitrile, and dried under vacuum.[13]

Sensitizer Synthesis. $Ru(dpp)_2Cl_2$ was prepared by a similar previously reported method.[14] 4,4′-diethyl ester-2,2′-bipyridine (deeb) was prepared from 4,4′-dimethyl-2,2′-bipyridine by the method of Oki and Morgan.[15]

(i) Bis(4,7-diphenyl-1,10-phenanthroline)(4,4′-diethyl ester-2,2′-bipyridine)ruthenium(II) Hexafluorophosphate, $[Ru(dpp)_2(deeb)](PF_6)_2$ (Ru-deeb). $Ru(dpp)_2Cl_2 \cdot 2H_2O$ (0.4 g, 0.46 mmol) and deeb (0.14 g, 0.467 mmol) were added to 30 mL of deaerated 1:1 EtOH/H_2O, and the mixture was refluxed under argon in the dark for 12 h. After the solution was cooled, the solvent was removed with a rotary evaporator. Distilled cold water (25 mL) was added, and the solution was filtered with a fine frit. About 2 mL of a saturated aqueous NH_4PF_6 solution was added to the filtrate, and a dark yellow precipitate formed immediately. The resulting precipitate was collected on a fine frit, washed with 10 mL of distilled water, and dried under vacuum. The compound was purified on alumina using 1:1 CH_3CN/diethyl ether as the eluent. Anal. Calcd for $C_{64}H_{48}N_6O_4P_2F_{12}$: C, 56.68; H, 3.54; N, 6.20. Found: C, 56.48; H, 3.63; N, 6.26. ^{1}H NMR δ, CD_3CN: 9.16 (1 H, d, $J = 3.6$ Hz), 8.28 (1 H, d, $J = 5.4$ Hz), 8.23 (1 H, s), 8.12 (1 H, d, $J = 5.4$ Hz), 8.10 (1 H, d, $J = 5.1$ Hz), 7.81(1 H, dd, $J = 5.7$ Hz), 7.76 (1 H, d, $J = 5.4$ Hz), 7.68 (1 H, d, $J = 3.6$ Hz), 7.65 (6 H, m), 7.62 (4 H, m), 7.60 (1 H, d, $J = 3.6$ Hz), 4.49 (2 H, q), 1.44 (3 H, t). IR: $\nu_{C=O} = 1722.7$ cm^{-1}. ESI-MS: *m*/*e* 1211.12 $(M - PF_6)^+$, 1065.20 $(M - 2PF_6)^+$, 1037.19 $(M - 2PF_6 - C_2H_4)^+$, 1009.17 $(M - 2PF_6 - 2C_2H_4)^+$, 533.2 $(M - 2PF_6)^{2+}$.

(ii) *cis*-Bis(4,7-diphenyl-1,10-phenanthroline)bis(4-ethyl esterpyridine)ruthenium(II) Hexafluorophosphate, $[cis\text{-}Ru(dpp)_2(eina)_2](PF_6)_2$ (Ru-eina). $Ru(dpp)_2Cl_2 \cdot 2H_2O$ (0.4 g, 0.46 mmol) and ethyl isonicotinate (eina) (1.5 mL, 10 mmol) were added to 30 mL of deareated 1:1 EtOH/H_2O, and the mixture was refluxed under argon in the dark for 24 h with vigorous stirring. After the solution was cooled, the solvent and unreacted ethyl isonicotinate were removed with a rotary evaporator. Distilled water (25 mL) was added, and the solution was filtered with a fine frit. About 2 mL of a saturated aqueous NH_4PF_6 solution was added to the filtrate. The resulting precipitate was collected on a fine frit that was subsequently washed with 10 mL of distilled water followed by 10 mL of diethyl ether, and was then dried under vacuum. The compound was purified on alumina in the dark using 2:1 CH_3CN/diethyl ether as the eluent. Anal. Calcd for $C_{64}H_{50}N_6O_4P_2F_{12}$: C, 56.50; H, 3.68; N, 6.19. Found: C, 56.30; H, 3.78; N, 6.18. ^{1}H NMR δ, CD_3CN: 9.42 (1 H, d, $J = 5.4$ Hz), 8.73 (2 H, dd, $J = 6.6$ Hz), 8.23 (1 H, d, $J = 5.4$ Hz), 8.155 (1 H, d, $J = 9.3$ Hz), 8.149 (1 H, d, $J = 5.7$ Hz), 8.06 (1 H, d, $J = 9.3$ Hz), 7.75 (2 H, dd, $J = 6.6$ Hz), 7.69 (6 H, m), 7.57 (4 H, m), 7.49 (1 H, d, $J = 3.6$ Hz), 4.36 (2 H, q), 1.36 (3 H, t). IR: $\nu_{C=O} = 1724.8$ cm^{-1}. ESI-MS: *m*/*e* 1212.81 $(M - PF_6)^+$.

Spectroscopy. (i) UV−Vis Spectroscopy. UV−visible ground-state absorption spectra were acquired using a Hewlett-Packard 8453 diode array spectrometer. For sensitized film measurements, an unsensitized TiO_2 film was used as the reference.

(ii) Transient Absorption. All transient absorption measurements were performed on samples that had been purged with nitrogen or argon gas. Transient absorption data were acquired with excitation from an ~8 ns, 532 nm laser pulse from a Surelite II Nd:YAG, Q-switched laser or a 417 nm laser pulse from a H_2-filled Raman shifter as previously described.[17] Briefly, a pulsed Xe lamp (150 W, Applied Photophysics) was positioned normal to the excitation beam, and was focused on the exposed TiO_2 surface. The excitation/probe orientation minimizes scattered light reaching the Hamamatsu R928 photomultiplier tube. The sample was also

(11) Qu, P.; Thompson, D. W.; Meyer, G. J. *Langmuir* **2000**, *16*, 4662.
(12) Liu, F.; Yang, M.; Meyer, G. J. In *Handbook of Sol Gel Science and Technology*; Sakka, S., Ed.; Kluwer Academic Publishers: Dordrecht, The Netherlands, 2005; Vol. II, p 399.
(13) Qu, P.; Meyer, G. J. *Langmuir* **2001**, *17*, 6720.
(14) Sullivan, B. P.; Salmon, D. J.; Meyer, T. J. *Inorg. Chem.* **1978**, *17*, 3334.
(15) Oki, A. R.; Morgan, R. J. *Synth. Commun.* **1995**, *25*, 4093.
(16) (a) Demas, J. N.; Crosby, G. A. *J. Phys. Chem.* **1971**, *75*, 991. (b) Casper, J. V.; Meyer, T. J. *J. Am. Chem. Soc.* **1983**, *105*, 5583.
(17) (a) Argazzi, R.; Bignozzi, C. A.; Hasselmann, G. M.; Meyer, G. J. *Inorg. Chem.* **1998**, *37*, 4533. (b) Bergeron, B. V.; Kelly, C. A.; Meyer, G. J. *Langmuir* **2003**, *19*, 8389.

protected from UV and IR light using suitable glass filters between the lamp and the sample. Scattered laser light was attenuated using the appropriate glass filter between the sample and monochromator. The absorption difference (typically an average of 40−50 laser pulses) was recorded as a function of wavelength before and after laser excitation.

(iii) Interfacial Electron Injection Quantum Yields (ϕ_{inj}). Injection quantum yields were determined by comparatively actinometry with a $Ru(bpy)_3Cl_2$/PMMA (polymethyl-methacrylate) film as a reference actinometer $\Delta\epsilon_{450} = (-1.0 \pm 0.09) \times 10^4\ M^{-1}\ cm^{-1}$ as previously described.[17] The ground-state−excited-state isosbestic points were determined by transient absorption of the sensitizers on ZrO_2 films. The $\Delta\epsilon$ between the oxidized sensitizer and ground-state sensitizer at the isosbestic point was determined by spectroelectrochemistry of the sensitizer in a 0.1 M TBAP/CH_3CN solution.

(iv) Photoluminescence. Steady-state corrected photoluminescence (PL) spectra were obtained with a Spex Fluorolog that had been calibrated with a standard tungsten−halogen lamp using procedures provided by the manufacturer. For sensitized films, the excitation beam was directed 45° to the film surface, and the emitted light was monitored from the front face of the sample. All photoluminescence measurements were performed on samples that had been purged with nitrogen or argon gas. Emission quantum yield, ϕ_{em}, was measured by the optically dilute technique using $Ru(bpy)_3^{2+}$ in water as a standard ($\phi_{em} = 0.042$),[16] eq 1.

$$\phi_{em} = (A_r/A_s)(I_r/I_s)(n_s/n_r)^2\phi_{em} \quad (1)$$

A_r and A_s, and I_s and I_r, are the absorption and integrated photoluminescence of the actinometer and sample, respectively, and n_r and n_s are the solvent refraction indexes for the actinometer and sample, respectively. Temperature-dependent steady-state PL spectra were acquired with an ISS-PC1 steady-state spectrofluorometer equipped with a Julabo VC temperature controller with a Julabo F20 cooler bath.

Time-resolved PL studies were performed with a Laser Photonics LN100/107 nitrogen-pumped dye laser as the excitation source. PL was collected at a right angle. A computer-interfaced LeCroy LT322 digital storage oscilloscope digitized the analogue signal from a Hamamatsu R928 photomultiplier tube. For solution studies, the traces were fit to a first-order kinetic model. Values for radiative and nonradiative constants, k_r and k_{nr}, respectively, were calculated from eqs 2 and 3 with the measured quantum yields and lifetimes.

$$\phi_{em} = k_r/(k_r + k_{nr}) \quad (2)$$

$$\phi_{em} = k_r/\tau \quad (3)$$

(v) Infrared Spectra. IR measurements were made by attenuated total reflectance (ATR) with a Golden Gate Single Reflection diamond ATR apparatus. The spectra were collected with a Nexus 670 Thermo-Nicolet FTIR spectrometer at a 4 cm^{-1} resolution.

(vi) NMR. ^1H NMR was performed on a Bruker 300 AMX or a Bruker AVANCE 400 FT-NMR spectrometer.

(vii) ESI-Mass Spectrometry. ESI-MS was carried out using a Thermo Finnigan LCQDeca Ion Trap mass spectrometer (San Jose, CA). Samples were dissolved in acetonitrile at a concentration of 0.4 mg/mL, to which was added 1% acetic acid as a buffer. The resulting sample solutions were then injected into the instrument by a syringe pump and fused silica capillary inlet with a liquid flow rate of 10 μL/min. The MS desolvation capillary was maintained at a temperature of 130 °C.

Electrochemistry. Cyclic voltammetry was performed in nitrogen-saturated 0.1 M TBAP/CH_3CN electrolyte. A BAS model CV27 potentiostat was used in a standard three-electrode arrangement with a Pt or glassy carbon working electrode, a Pt gauze counter electrode, and a Ag/AgCl or $Ag/AgNO_3$ reference electrode. Cyclic voltammetry of the sensitizers bound to TiO_2 on a conductive glass was performed in a similar manner, with the sensitized TiO_2 film as the working electrode.

(i) Photoelectrochemistry. Photoelectrochemical and incident-photon-to-current conversion efficiency (IPCE) measurements were performed in a two-electrode sandwich cell arrangement as previously described.[11] The IPCE was calculated using eq 4

$$\mathrm{IPCE} = (1240 i_{ph})/(P\lambda) \quad (4)$$

where i_{ph} is the photocurrent per unit area in $\mu A/cm^2$ at incident wavelength λ (nm) and P is the incident irradiation per unit area in $\mu W/cm^2$, determined with a UDT 260 optometer.

(ii) Spectroelectrochemistry. Spectroelectrochemistry was performed for sensitizers in a 0.1 M TBAP/CH_3CN solution in a locally designed 0.1 cm light path quartz cuvette. A wide area Pt mesh electrode was used as the working electrode while a $Ag/AgNO_3$ reference electrode and a Pt gauze auxiliary electrode were also employed. Potentials were applied using a PAR model 173 potentiostat. Argon was bubbled gently during the experiment. UV−vis spectra were recorded with a Hewlett-Packard 8453 diode array spectrometer.

Elemental Analysis. Elemental analyses were obtained from Atlantic Microlab, Inc., Atlanta, GA.

Results

The Ru(II) compounds were synthesized by standard techniques, and were satisfactorily characterized by ^1H NMR, elemental analysis, electrochemistry, and photophysical measurements. In cyclic voltammetry experiments, both compounds exhibited a single quasi-reversible $Ru^{III/II}$ wave and ligand-localized waves corresponding to the sequential reductions of the diimine ligands. The redox chemistry is termed quasi-reversible because the anodic and cathodic currents were approximately equal but the peak-to-peak separation was typically ~80 mV in fluid solution over scan rates of 10−100 mV/s.[18]

The $Ru^{III/II}$ reduction potentials, $E_{1/2}(Ru^{III/II})$, of **Ru-deeb** and **Ru-eina** were ~1.3 V, which is characteristic of ruthenium polypyridyl compounds.[19] The first ligand-based reduction, $E_{1/2}(Ru^{2+/+})$, of **Ru-deeb** occurred at a potential close to or more positive than the corresponding reference compounds, $[Ru(deeb)_3]^{2+}$ and $[Ru(dpp)_3]^{2+}$, respectively.[20] This wave was assigned to the reduction of the coordinated deeb ligand. The sequential reductions of the two dpp ligands were observed at more negative potentials. By comparison with $[Ru(dpp)_3]^{2+}$ and literature reports on Ru(II) compounds coordinated to pyridine ligands,[11,19] the dpp ligands of **Ru-eina** were reduced and the reduction of eina was not observed in the potential range studied. The metal- and ligand-based

(18) Bard, A. J.; Faulkner, L. R. *Electrochemical Methods: Fundamentals and Applications*, 2nd ed.; John Wiley & Sons: New York, 2001.
(19) Juris, A.; Balzani, V.; Barigelletti, F.; Campagna, S.; Belser, P.; Zelewsky, A. V. *Coord. Chem. Rev.* **1988**, *84*, 85.
(20) (a) Lin, C. T.; Boettcher, W.; Chou, M.; Creutz, C.; Sutin, N. *J. Am. Chem. Soc.* **1976**, *98*, 6536. (b) Elliott, C. M.; Hershenhart, E. J. *J. Am. Chem. Soc.* **1982**, *104*, 7519. (c) McCord, P.; Bard, A. J. *J. Electroanal. Chem.* **1991**, *318*, 91.

Table 1. Reduction Potentials[a] and Photophysical Properties of **Ru-deeb** and **Ru-eina**

compound	$E_{1/2}$ (V) $Ru^{III/II}$	$Ru^{2+/+}$	$Ru^{+/0}$	$Ru^{0/-}$	$\lambda_{abs,max}$ (nm)	$\lambda_{em,max}$ (cm^{-1}) 298 K	77 K[b]	τ (ns)	ϕ_{em}	k_r ($s^{-1} \times 10^4$)	k_{nr} ($s^{-1} \times 10^6$)
Ru-deeb	1.38	−1.18	−1.33	−1.49	490	14 880	15 700	780	0.067	8.68	1.20
Ru-eina	1.34	−1.35	−1.51	N/A	470		17 000	<10		N/A	N/A

[a] Reduction potential measured in 0.1 M TBAP/CH_3CN electrolyte. The potentials given are versus Ag/AgCl. [b] Data measured in a 4:1 EtOH/MeOH glass at 77 K.

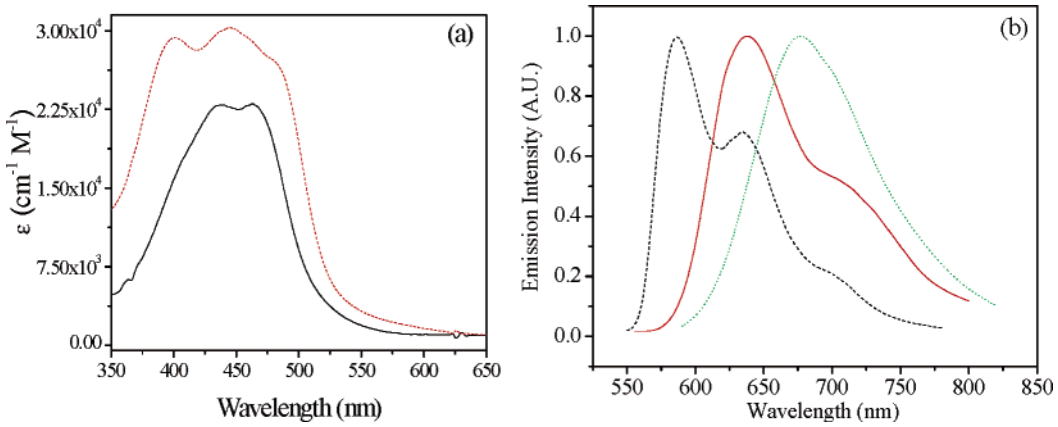

Figure 1. (a) Absorption spectra of **Ru-deeb** (- - -) and **Ru-eina** (—) in acetonitrile. (b) Normalized photoluminescence spectra of **Ru-deeb** in acetonitrile at room temperature (- - -) and of **Ru-deeb** (—) and **Ru-eina** (···) in a 4:1 mixture of EtOH and MeOH (v/v) at 77 K.

Table 2. Photophysical Properties and Injection Quantum Yields for Sensitizers Anchored to TiO_2[a]

compound	untreated TiO_2 λ_{abs} (nm)	λ_{em} (nm)	$E_{1/2}(Ru^{III/II*})$ (V)	pH = 1 TiO_2 λ_{ab} (nm)	λ_{em} (nm)	$E_{1/2}(Ru^{III/II*})$ (V)	on ZrO_2 λ_{abs} (nm)	λ_{em} (nm)	ϕ_{inj} pH = 1 TiO_2	pH = 3 TiO_2	pH = 5 TiO_2	pH =12 TiO_2	TiO_2
Ru-deeb	475	631	−0.81	490	675	−0.77	475	643	0.96	0.69	0.28	≤0.05	0.17
Ru-eina	460	612	−0.85	475	618	−0.80	462	614	0.82	0.50	0.21	≤0.05	0.19

[a] All measurements were performed in neat acetonitrile or 0.1 M TBAP/CH_3CN electrolyte. The potentials given are versus Ag/AgCl.

reduction potentials of **Ru-deeb** and **Ru-eina** in 0.1 M $TBAClO_4$ acetonitrile electrolyte are provided in Table 1.

The Ru(III/II) reduction potentials of **Ru-deeb** and **Ru-eina** anchored to TiO_2 were within 50 mV of those measured in fluid solution. This is consistent with previous reports of ruthenium polypyridyl compounds with dcb or deeb ligands.[8,13] When the interfacial proton concentration was varied with surface pretreatment, the $E_{1/2}(Ru^{III/II})$ was found to shift about 10 mV per pH unit in a negative direction for both **Ru-deeb** and **Ru-eina**.

The **Ru-deeb** and **Ru-eina** absorption spectra in acetonitrile displayed a broad band in the visible region (400−500 nm) that is typical of MLCT transitions, Figure 1a. Room-temperature photoluminescence (PL) was observed for **Ru-deeb** in argon-saturated acetonitrile, Figure 1b. Excitation and 1-*T*, where *T* is the transmittance, spectra were in good agreement. The excited state decayed with first-order kinetics, τ = 780 ns, that were independent of the excitation or monitoring wavelength. No detectable emission was observed from **Ru-eina** under these same conditions.[21] Both compounds emitted strongly in EtOH/MeOH (4:1 v/v) glass at 77 K with a vibronic progression ($\nu \sim 1300$ cm^{-1}) characteristic of ruthenium polypyridyl excited states.[22] The photoluminescence maximum of **Ru-deeb** shifted by 820 cm^{-1} from 14 880 cm^{-1} at 298 K to 15 700 cm^{-1} at 77 K.

The photophysical properties of **Ru-deeb** and **Ru-eina** are summarized in Table 1.

Both compounds displayed room-temperature photoluminescence when anchored to TiO_2 in acetonitrile, Table 2. The photoluminescence intensity and maximum were found to be dependent on the surface acidity. On acid-pretreated TiO_2, a weak red-shifted emission was generally observed. On basic TiO_2, a strong emitting and long-lived excited state was observed. Nearly identical photoluminescence spectra were observed for the compounds anchored to TiO_2 and ZrO_2.

The excited-state reduction potential, $E_{1/2}(Ru^{III/II*})$, was related to the ground-state reduction potential by $E_{1/2}(Ru^{III/II*}) = E_{1/2}(Ru^{III/II}) - \Delta G_{es}$. The free energy stored in the photoluminescent excited state (ΔG_{es}) was estimated from a tangent line drawn on the high-energy side of the corrected PL spectrum of the surface-bound compounds in neat acetonitrile.[1] The excited-state reduction potentials $E_{1/2}(Ru^{III/II*})$

(21) (a) Ford, P. C.; Stuermer, D. H.; McDonald, D. P. *J. Am. Chem. Soc.* **1969**, *91*, 6209. (b) Durante, V. A.; Ford, P. C. *Inorg. Chem.* **1979**, *18*, 588. (c) Durham, B.; Caspar, J. V.; Nagle, J. K.; Meyer, T. J. *J. Am. Chem. Soc.* **1982**, *104*, 4803. (d) Coe, B. J.; Meyer, T. J.; White, P. S. *Inorg. Chem.* **1993**, *32*, 4012.

(22) Thompson, D. W.; Schoonover, J. R.; Graff, D. K.; Fleming, C. N.; Meyer, T. J. *J. Photochem. Photobiol., A* **2000**, *137*, 131.

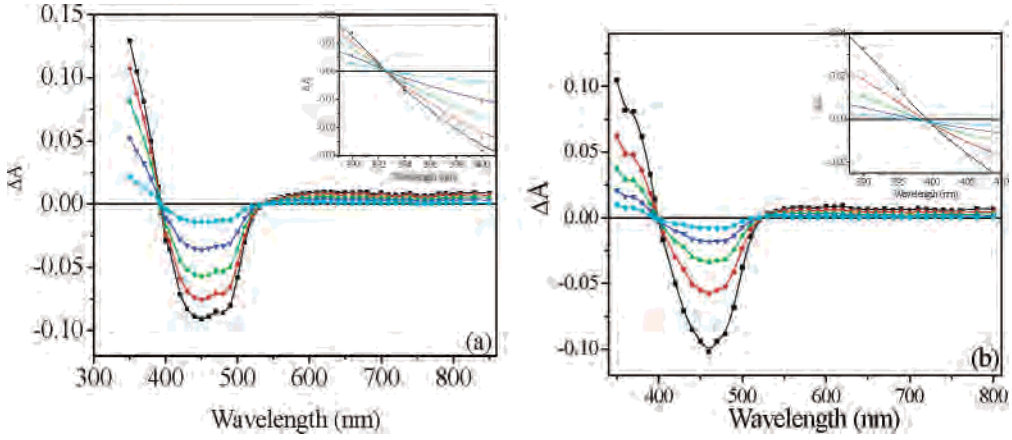

Figure 2. Time-resolved absorption difference spectra recorded after pulsed 417 nm light excitation (~11 mJ/pulse, 8 ns fwhm) of **Ru-deeb**: (a) in acetonitrile solution, and (b) on ZrO_2. Data were recorded at 0 ns (■), 200 ns (●), 500 ns (▲), 1 μs (▼), and 2 μs (◆). Isosbestic points are shown in the insets.

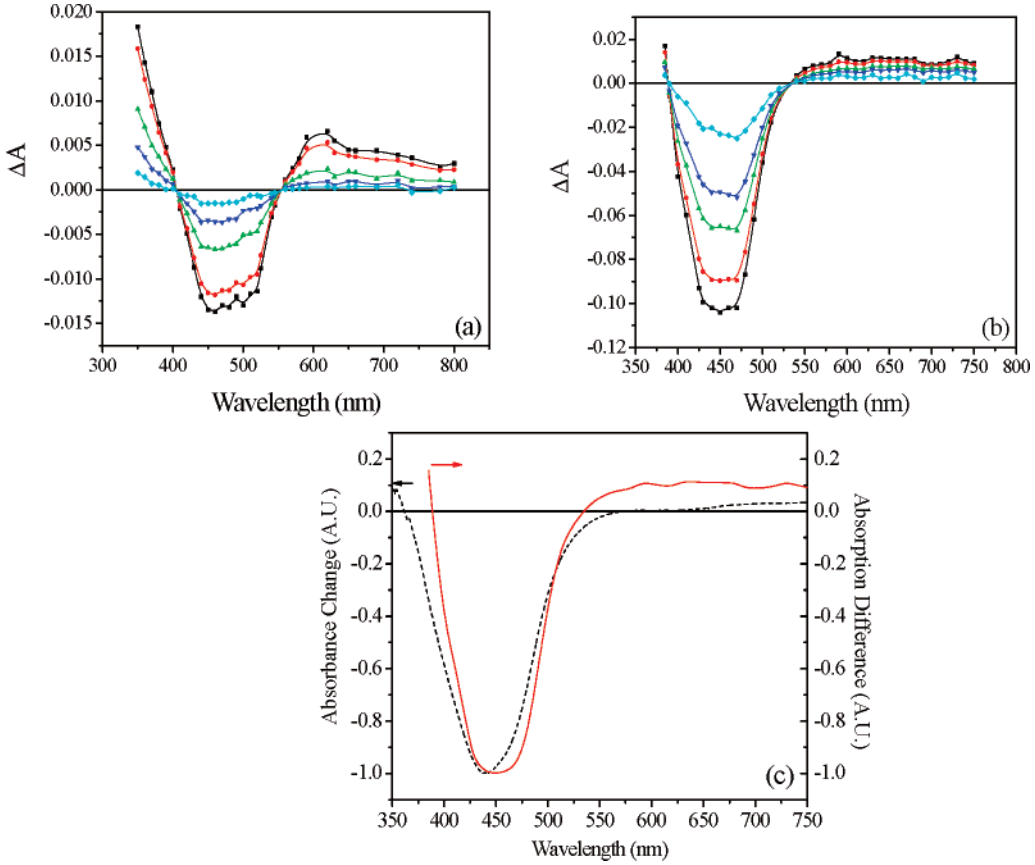

Figure 3. Time-resolved absorption difference spectra recorded after pulsed light excitation (417 nm, ~11 mJ/pulse, 8 ns fwhm) of **Ru-eina** on (a) ZrO_2 and (b) pH = 1 pretreated TiO_2. Data were recorded at 0 ns (■), 50 ns (●), 250 ns (▲), 500 ns (▼), and 1 μs (◆) in (a), and at 0 ns (■), 250 ns (●), 1 μs (▲), 2 μs (▼), and 10 μs (◆) in (b). Shown in (c) is the absorption difference spectrum obtained from (b) at a 2 μs delay (—) and the absorbance spectrum obtained by subtraction of the Ru^{II} absorption spectrum from that of Ru^{III} (- - -).

were found to decrease by about 5 mV/pH with increasing pH.

Time-resolved absorption difference spectra of **Ru-deeb** in acetonitrile and on ZrO_2 were qualitatively similar and are shown in Figure 2.[23] The spectra were assigned to the MLCT excited state, with characteristic absorptions of the reduced ligand below 400 nm, and a bleach of the MLCT band centered at ~450 nm. Isosbestic points were observed at 392.5 and 537 nm in solution (Figure 2a inset), and at 399.5 and 526 nm on ZrO_2 (Figure 2b inset). First-order kinetic fits of single-wavelength transient absorption data in solution yielded, within experimental error, the same lifetimes as those extracted from time-resolved PL measurements.

The excited-state lifetime of **Ru-eina** in fluid acetonitrile could not be time-resolved, consistent with $\tau < 10$ ns. The transient absorption difference spectra observed after pulsed-light excitation of **Ru-eina**/ZrO_2 were assigned to the MLCT excited state, Figure 3a. A strong positive absorption band

(23) Kumar, C. V.; Barton, J. K.; Gould, I. R.; Turro, N. J.; Houten, J. V. *Inorg. Chem.* **1988**, *27*, 648.

centered at ~600 nm was observed.[23] This band was absent on pH = 1 pretreated TiO_2, and the transient difference spectrum was assigned to the interfacial charge-separated state $Ru^{III}/TiO_2(e^-)$, Figure 3b.

Spectroelectrochemistry was employed to simulate the transient absorption spectra observed in acidic TiO_2. A representative example for **Ru-eina**/TiO_2 is shown in Figure 3c. The **Ru-eina**/TiO_2 was oxidized to Ru^{III} at +1.6 V vs Ag/AgCl in 0.1 M $TBAClO_4$ acetonitrile electrolyte. Upon oxidation, an absorbance increase below 370 nm, a loss at 370−550 nm, and a slight increase above 625 nm were observed. The absorbance change, $Ru^{III} - Ru^{II}$, shown in Figure 3c as a dashed line, closely resembled the spectrum observed transiently, Figure 3c solid line. The spectroelectrochemical data show slightly less absorption at long wavelengths, $\lambda > 550$ nm, and this is likely due to some contributions from the injected electron in the transient absorption spectra.[24] Similar results were obtained for **Ru-deeb** on pH = 1 TiO_2.

The formation of the oxidized sensitizers could not be time resolved, consistent with rapid interfacial electron injection, $k_{inj} > 10^8\ s^{-1}$. Interfacial charge recombination was well described by a second-order kinetic model with a non-zero baseline in the time interval of 0−5 μs, eq 5

$$\Delta A(t) = \frac{\Delta A_0 - \Delta A_f}{1 + (k/\Delta\epsilon l)t(\Delta A_0 - \Delta A_f)} \qquad (5)$$

where $\Delta A(t)$ is the absorbance difference at time t, $\Delta\epsilon$ is the molar extinction coefficient change between the oxidized and ground-state compound at the wavelength monitored, l is the optical path length, ΔA_0 is the absorbance change extrapolated to time zero, ΔA_f is the absorbance change at 5 μs, and k is the second-order rate constant.[25] The observed average rate constant, $k_{obs} = (1.2 \pm 0.3) \times 10^8\ s^{-1}$, for charge recombination was found to be independent of the sensitizer and the monitoring wavelength, and was the apparent driving force over the 11 pH unit change in surface pretreatment conditions. The full recovery of the initial spectrum required milliseconds, and was not quantified in detail.

The injection quantum yield, ϕ_{inj}, was determined by comparative actinometry using $Ru(bpy)_3^{2+}$/PMMA film as a standard.[17] We monitored at the excited-state−ground-state isosbestic points determined on ZrO_2, and therefore the signal was not complicated by excited-state absorption, and the injection quantum yield could be obtained. The injection quantum yields were found to depend on the nature of the sensitizer and surface pretreatment of TiO_2. On acidic TiO_2, the TA spectra were mainly from the $Ru^{III}/TiO_2(e^-)$ charge-separated states, whereas on basic TiO_2, the MLCT excited state was predominantly observed and a much lower injection quantum yield was obtained. Table 2 shows quantitative ϕ_{inj} data for **Ru-deeb** and **Ru-eina** on different pH pretreated TiO_2 surfaces.

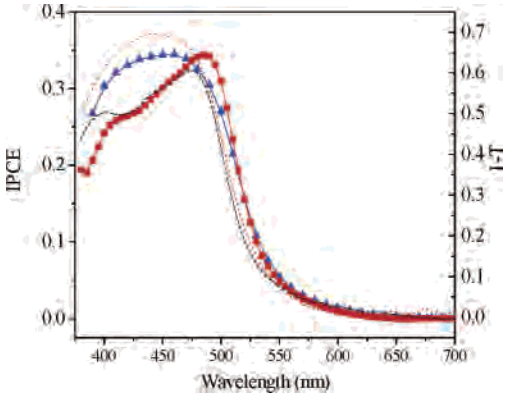

Figure 4. Incident-photon-to-current conversion efficiency (IPCE) of **Ru-deeb** (■) and **Ru-eina** (▲) on TiO_2/FTO with 0.5 M LiI and 0.05 M I_2 in acetonitrile. Also shown are the corresponding absorptance (1-T) spectra of **Ru-deeb** (- - -) and **Ru-eina** (···).

Figure 4 shows the incident-photon-to-current conversion efficiency (IPCE) versus excitation wavelength for compounds **Ru-deeb** and **Ru-eina** on TiO_2/FTO with 0.5 M LiI/0.05 M I_2 acetonitrile as electrolyte. The photocurrent action spectra and absorptance spectra agreed very well within experimental error. An ~5-fold decrease in IPCE was observed if tetrabutylammonium cation was used instead of lithium.

Steady-state PL intensities of **Ru-eina** anchored to TiO_2 films were temperature-dependent. Increasing the temperature from 0 to 50 °C resulted in an ~4-fold decrease in the PL intensity. The intensity could be restored by lowering the temperature back to zero. Typical time-resolved PL decays on ZrO_2, TiO_2, and pH = 2 pretreated TiO_2 are shown in Figure 5. The PL decays were nonexponential and were well-described by a parallel first- and second-order kinetic model, eqs 6 and 7

$$\mathrm{PLI}(t) = B\left(\frac{k_1 \exp(-k_1 t)}{k_1 + p - p\exp(-k_1 t)}\right) \qquad (6)$$

$$p = k_2[Ru^{2+*}]_{t=0} \qquad (7)$$

where k_1 is a first-order rate constant analogous to solution and B is a constant. The parameter p is the product of the observed second-order rate constant, k_2, and the initial concentration of ruthenium excited states, $[Ru^{2+*}]_{t=0}$.[26] Arrhenius analysis of the first-order rate constant gave an apparent activation energy of 1700 ± 100 cm^{-1} that was substrate-independent (ZrO_2 or TiO_2). On pH = 2 pretreated TiO_2, **Ru-eina** displayed static and dynamic quenching with increased temperature as reflected by changes in lifetimes and the initial amplitudes. For **Ru-deeb**, only a slight temperature-dependent dynamic quenching was observed.

The electron injection quantum yields for **Ru-eina** on pH = 1 and 2 pretreated TiO_2 in neat acetonitrile were temperature-dependent, and typically increased ~30% when the temperature decreased from 60 to 0 °C, Figure 6. This behavior was reversible with temperature. There was no

(24) Rothenberger, G.; Fitzmaurice, D.; Grätzel, M. *J. Phys. Chem.* **1992**, *96*, 5983.
(25) Kelly, C. A.; Thompson, D. W.; Farzad, F.; Stipkala, J. M.; Meyer, G. J. *Langmuir* **1999**, *15*, 7047.
(26) Kelly, C. A.; Farzad, F.; Thompson, D. W.; Meyer, G. J. *Langmuir* **1999**, *15*, 731.

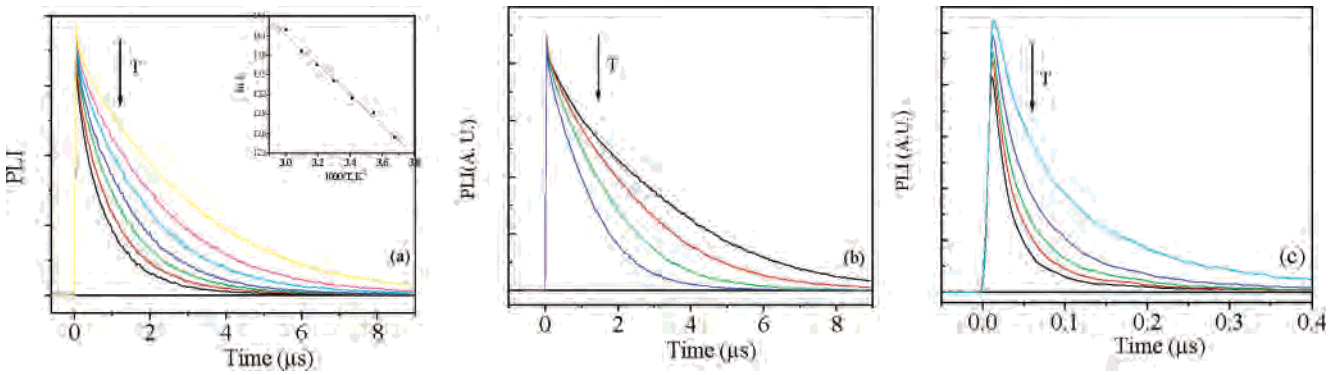

Figure 5. Time-resolved PL decays of compound **Ru-eina** on (a) ZrO_2, (b) TiO_2, and (c) pH = 2 TiO_2 in neat acetonitrile as a function of temperature. The arrows indicate the direction of the increase of temperature. The inset in (a) displays a representative Arrhenius plot of the data from which an activation energy of 1700 ± 100 cm^{-1} was abstracted.

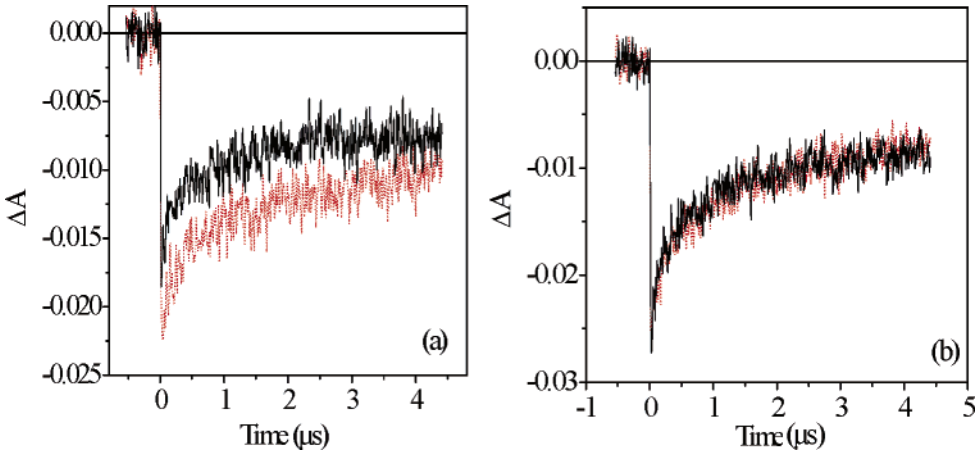

Figure 6. Time-resolved absorption transients recorded after pulsed-light excitation (417 nm, ~11 mJ/pulse, 8 ns fwhm) of (a) **Ru-eina** on pH = 2 pretreated TiO_2 and (b) **Ru-deeb** on pH = 2 pretreated TiO_2 at 273 K (red dots) and 333 K (black line).

detectable temperature-dependent injection when **Ru-eina** was anchored to pH = 5 pretreated or untreated TiO_2. Injection yields were also found to be temperature-independent for **Ru-deeb** from 60 to 0 °C under all conditions investigated.

Discussion

The two heteroleptic Ru(II) polypyridyl sensitizers allowed remote and adjacent interfacial electron-transfer processes to be studied, Scheme 1. Aqueous acid pretreatments were used to tune the energetic position of the conduction band edge relative to that of the excited sensitizer. Proton adsorption/intercalation on metal oxide semiconductors is well-known to shift the flat-band potential positive on an electrochemical scale (i.e., away from the vacuum level) by 59 mV/pH.[27] Several groups have found that equilibration with aqueous solutions has a similar influence on TiO_2 energetics in organic solvents.[13,28] The sensitizer potentials also shift in the same direction with the interfacial proton concentration,[29] but the $Ru^{III/II*}$ shift quantified here was smaller, <10 mV/pH for **Ru-deeb**/TiO_2 and **Ru-eina**/TiO_2. Thus it was possible to systematically tune the TiO_2 conduction band edge relative to the sensitizer reduction potential.

The aqueous pretreatments studied here exerted a profound influence on the interfacial electron injection quantum yields, changing from $\phi_{inj} < 0.05$ at pH 12 to $\phi_{inj} \sim 1$ at pH 1. This finding allowed us to quantify the excited states and interfacial electron transfer under similar experimental conditions. Below we provide details of these findings and discuss their relevance to literature reports and solar energy conversion.

^{3}MLCT Excited States. The visible absorption of the ruthenium polypyridyl compounds was largely preserved upon surface binding. The excited-state behavior was significantly different, particularly for **Ru-eina**. This compound was nonemissive and photochemically unstable, with a short excited-state lifetime in fluid solution. Upon binding to ZrO_2 or basic TiO_2, the compound became highly luminescent with long-lived excited states. This behavior is reminiscent of *cis*-$Ru(bpy)_2(py)_2^{2+}$, where py is pyridine, which is nonemissive in fluid solution but emits strongly in solid-state media.[11,30] The presence of low-lying ligand field states that are antibonding with respect to metal−ligand bonds lowers the

(27) Gomes, W. P.; Cardon, F. *Prog. Surf. Sci.* **1982**, *12*, 155.
(28) Wang, Z. S.; Yamaguchi, T.; Sugihara, H.; Arakawa, H. *Langmuir* **2005**, *21*, 4272.
(29) (a) Zaban, A.; Ferrere, S.; Sprague, J.; Gregg, B. A. *J. Phys. Chem. B* **1997**, *101*, 55. (b) Zaban, A.; Ferrere, S.; Gregg, B. A. *J. Phys. Chem. B* **1998**, *102*, 452.
(30) (a) Durham, B.; Walsh, J. L.; Carter, C. L.; Meyer, T. J. *Inorg. Chem.* **1980**, *19*, 860. (b) Adelt, M.; Devenney, M.; Meyer, T. J.; Thompson, D. W.; Treadway, J. A. *Inorg. Chem.* **1998**, *37*, 2616.

excited-state lifetime and results in photochemical ligand loss. Upon surface binding, the MLCT → LF internal conversion activation energy for **Ru-eina**/TiO_2 or **Ru-eina**/ZrO_2 increased to 1700 ± 100 cm^{-1}, and the sensitizer became photostable with long-lived excited states. We note that McCusker et al. have shown that the phenyl rings in related Ru(II) bipyridyl compounds become more coplanar with the bipyridyl rings in the excited state.[31] This increased delocalization may also contribute to the long excited-state lifetime of the **Ru-eina**/TiO_2.

The term lifetime is used rather loosely, as excited-state decay was nonexponential on these nanocrystalline surfaces. The time-resolved data were well-described by a parallel first- and second-order kinetic model. The first-order process represents the sum of the unimolecular radiative and nonradiative rate constants. The second-order component arises from intermolecular energy transfer across the semiconductor surfaces that ultimately lead to bimolecular triplet−triplet annihilation reactions. This behavior has previously been characterized for related Ru(II)-sensitized materials, and direct evidence for energy transfer came from TiO_2 materials cosensitized with Ru(II) and Os(II).[26,32]

It is now reasonably well established that the excited state of $Ru(bpy)_3^{2+*}$ is localized on a single ligand in fluid solution.[33,34] A question that arises for heteroleptic compounds concerns which ligand the excited state is localized on. The assignment of excited-state localization on the dpp ligand in **Ru-eina*** is relatively unambiguous, as the eina π^* levels are at much higher energy.[21,35,36] Comparisons with literature data indicate that the excited state of **Ru-deeb** is localized on the deeb ligand. The electrochemical[35] data support these assignments in fluid solution, and the spectroscopic data indicate that this is maintained when the sensitizers are anchored to TiO_2 or ZrO_2. Thus interfacial injection from the emissive excited state is indeed remote for **Ru-eina**/TiO_2 and adjacent for **Ru-deeb**/TiO_2, Scheme 1.

Interfacial Electron Transfer. The photoelectrochemical results provide strong evidence for efficient remote excited-state interfacial injection. The incident-photon-to-current efficiency (IPCE) is the product of three terms: the light-harvesting efficiency, the electron injection quantum yield (ϕ_{inj}), and the efficiency of electron collection in the external circuit.[1] The light-harvesting term can be directly assessed from the absorptance spectrum of the surface-bound sensitizers. For internal comparisons it is sometimes useful to contrast the absorbed photon-to-current efficiencies, which are approximately the same for the two sensitizers. Since both sensitizers have very positive $Ru^{III/II}$ reduction potentials,

Scheme 2

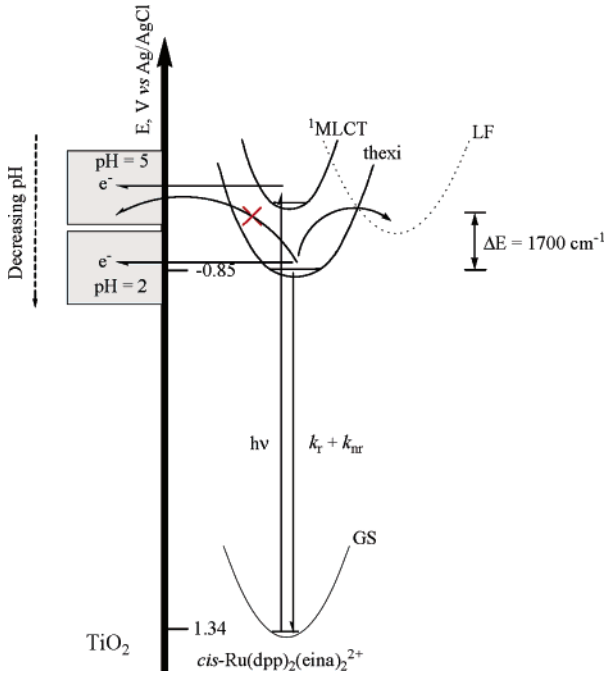

regeneration by iodide oxidation is expected to be very rapid, and the injected electrons should be collected with comparable efficiencies.[1] Thus photocurrent action spectra like those shown in Figure 4 are consistent with $\phi_{inj} > 0.5$.

The electron injection quantum yields were measured directly in neat acetonitrile by nanosecond comparative actinometry.[17] The ϕ_{inj} values for **Ru-eina**/TiO_2 were typically about 20% smaller than those of **Ru-deeb**/TiO_2 under similar conditions. With acidic pretreatments, the ϕ_{inj} values for **Ru-eina**/TiO_2 were greater than 80%. This is larger than the value inferred from the photocurrent action spectra, and may indicate that the iodide/iodine electrolyte is lowering injection yields in the operational solar cell.

The electron injection rate constants for both **Ru-deeb**/TiO_2 and **Ru-eina**/TiO_2 could not be time resolved, consistent with $k_{inj} > 10^8$ s^{-1}. The second-order rate constant for charge recombination between the electron in TiO_2 and the oxidized sensitizer was found to be sensitizer-independent. The recombination rate constant showed no measurable dependence on surface acidity, consistent with previous studies.[37]

The electron injection quantum yields for **Ru-eina** on pH = 1 and pH = 2 pretreated TiO_2 were found to increase by ~30% when the temperature was decreased from 60 to 0 °C. An increase in ϕ_{inj} with decreased temperature is opposite to what one would expect for excited-state electron injection as described by Gerischer.[1,38] To account for this behavior, a model is proposed wherein a branching ratio exists between electron injection from the thermally equilibrated excited (thexi) state and activated crossing to ligand-field states, Scheme 2. Under more basic TiO_2 conditions, injection from the thexi state is thermodynamically unfavored, and deac-

(31) (a) Damrauer, N. H.; Boussie, T. R.; Devenney, M.; McCusker, J. K. *J. Am. Chem. Soc.* **1997**, *119*, 8253. (b) Curtright, A. E.; McCusker, J. K. *J. Phys. Chem. A* **1999**, *103*, 7032.
(32) Farzad, F.; Thompson, D. W.; Kelly, C. A.; Meyer, G. J. *J. Am. Chem. Soc.* **1999**, *121*, 5577.
(33) (a) Meyer, T. J. *Pure Appl. Chem.* **1986**, *58*, 1576. (b) Kober, E. M.; Caspar, J. V.; Lumpkin, R. S.; Meyer, T. J. *J. Phys. Chem.* **1986**, *90*, 3722.
(34) Dallinger, R. F.; Woodruff, W. H. *J. Am. Chem. Soc.* **1979**, *101*, 4391.
(35) Lever, A. B. P. *Inorg. Chem.* **1990**, *29*, 3415.
(36) Liu, F.; Meyer, G. J. *Inorg. Chem.* **2003**, *42*, 7351.
(37) Yan, S. G.; Hupp, J. T. *J. Phys. Chem. B* **1998**, *102*, 1745.
(38) (a) Gerischer, H. *Photochem. Photobiol.* **1972**, *16*, 243. (b) Gerischer, H.; Willig, F. *Top. Curr. Chem.* **1976**, *61*, 31. (c) Gerischer, H. *Pure Appl. Chem.* **1980**, *52*, 2649.

tivation through the ligand-field (LF) states lowers the injection quantum yield. We emphasize that this model does not require that a well-defined singlet excited state exist, and is just as easily explained by injection from upper vibrational levels of the thexi states. We have invoked spin in Scheme 2 to be consistent with models proposed from ultrafast studies of related sensitized materials.[1,5]

It is interesting to consider the following question: under what conditions does activated interfacial electron injection from the thexi state occur? Gerischer theory indicates that interfacial electron injection should be activated when the sensitizer excited-state reduction potential is less than twice the reorganization energy above the conduction band edge.[38] We specifically looked for this behavior with **Ru-deeb**/TiO_2, as its excited-state reduction potential is very similar to that of **Ru-eina**/TiO_2, and complications from ligand-field states are unlikely. However, under all conditions of pH and temperature examined, we observed instrument-response-limited, temperature-independent electron injection yields. Indeed, we are unaware of any literature evidence for activated electron injection at sensitized semiconductor interfaces, although it is theoretically predicted. Our current thinking for **Ru-deeb**/TiO_2 is that injection from upper excited states masks this behavior. In future studies, we will look for activated electron injection from sensitizers that have weaker electronic interactions with the semiconductor.

Conclusion

In summary, interfacial proton concentration has been effectively employed to tune the conduction band edge of nanocrystalline TiO_2 films relative to the reduction potentials of the sensitizer. On untreated and basic TiO_2, long-lived excited states were observed, whereas on acidic TiO_2, the excited state was quenched and electron injection predominated. Excited-state injection from a remote ligand was found to occur with high quantum yields that could be tuned with temperature. A model is proposed to account for the temperature dependence wherein the thermally equilibrated excited state can deactivate through competitive electron injection and internal conversion (to LF excited states) pathways. Activated electron injection from a sensitizer without low-lying ligand field states has been predicted theoretically but was not observed. Evaluation of the molecular factors that influence interfacial electron injection across sensitized-semiconductor interfaces continues to be an important goal.

Acknowledgment. The Division of Chemical Sciences, Office of Basic Energy Sciences, Office of Energy Research, U.S. Department of Energy, is gratefully acknowledged for research support.

IC0513336